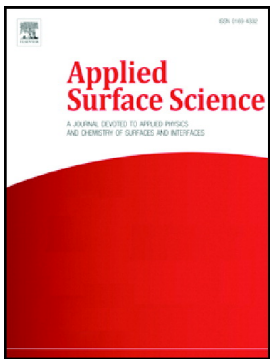

SiOx by magnetron sputtered revisited: Tailoring the photonic properties of multilayers

Aurelio García-Valenzuela, Rafael Alvarez, Juan Pedro Espinós, Victor Rico, Jorge Gil-Rostra, Alberto Palmero, Agustin R. Gonzalez-Elipe

PII: S0169-4332(19)31582-X
DOI: https://doi.org/10.1016/j.apsusc.2019.05.273
Reference: APSUSC 42860

To appear in: *Applied Surface Science*

Received date: 25 February 2019
Revised date: 22 May 2019
Accepted date: 23 May 2019

Please cite this article as: A. García-Valenzuela, R. Alvarez, J.P. Espinós, et al., SiOx by magnetron sputtered revisited: Tailoring the photonic properties of multilayers, Applied Surface Science, https://doi.org/10.1016/j.apsusc.2019.05.273

SiOx by magnetron sputtered revisited: tailoring the photonic properties of multilayers

Aurelio García-Valenzuela,[1] Rafael Alvarez,[1,2] Juan Pedro Espinós,[1] Victor Rico,[1] Jorge Gil-Rostra,[1] Alberto Palmero,[1*] Agustin R. Gonzalez-Elipe[1*]

1.-Laboratory of Nanotechology on Surfaces. Instituto de Ciencia de Materiales de Sevilla [CSIC-Univ. Seville]. Avda. Américo Vespucio 49. 41092 Sevilla. Spain.
2.- Departamento de Física Aplicada I. Escuela Politécnica Superior, Universidad de Sevilla. c/ Virgen de África 7, 41011, Seville, Spain

**arge@icmse.csic.es; *alberto.palmero@csic.es*

Keywords: SiOx thin films, magnetron sputtering, OAD, NIR optofluidics, label free photonic sensor

Traditionally porous silicon based photonic structures have been prepared by electrochemically etching of silicon. In this work, porous multilayers of nanocolumnar SiOx and SiO2 thin films acting as near infrared (NIR) 1D-photonic nanostructures are prepared by magnetron sputtering deposition at oblique angles (MS-OA). Simultaneous control of porosity and stoichiometry of the stacked films is achieved by adjusting the deposition angle and oxygen partial pressure according to a parametric formula. This new methodologoy is proved for the synthesis of SiOx thin films with x close to 0.4, 0.8, 1.2, 1.6 and nanostructures varying from compact (at 0° deposition angle) to highly porous and nanocolumnar (at 70º and 85° deposition angles). The strict control of composition, structure and nanostructure provided by this technique permits a fine tuning of the absorption edge and refraction index at 1500 nm of the porous films and their manufacturing in the form of SiOx-SiO_2 porous multilayers acting as near infrared (NIR)

1D-photonic structures with well-defined optofluidic responses. Liquid tunable NIR Bragg mirrors and Bragg microcavities for liquid sensing applications are presented as proof of concept of the possibilities of this MS-OAD manufacturing method as an alternative to the conventional electrochemical procedure of silicon based photonic structures.

1. Introduction

Porous silicon oxide is a classical material for the fabrication of self-standing optofluidic actuation and/or interrogation an sensing devices and as such it has been widely used for a large set of sensing and responsive applications including label free sensing and detection of biomolecules and tumor necrosis factors [1-4]. Current methods of fabrication of these porous silicon devices rely on chemical routes involving electrochemical treatments and thermal annealing at high temperatures that may hamper their straightforward incorporation into microfluidic systems. A motivation of the present paper is to apply thin film synthesis routes to directly deposit porous nanostructures made of silicon oxide onto any kind of substrates at room temperature. Key feature of the developed approach is the controlled manufacturing of SiO_x($x<2$) thin films by magnetron sputtering. Thin films of this material have been studied for decades due to their outstanding optical and electrical properties.[5-9] Recently, SiO_x nanowires have been proposed as refractive index sensing devices,[10] while in the form of stacked layers and porous films this material is utilized for the fabrication of Li battery electrodes.[11,12] Compact SiO_x thin films have been fabricated by various methods, including evaporation [13-15] thermal chemical vapor deposition (CVD), [16,17] or magnetron sputtering (MS).[18-20] Radio frequency reactive MS was profusely utilized by Habraken et al. for the deposition of SiOx thin films.[21-26] Besides

determining the best deposition conditions to achieved a precise control over stoichiometry, these authors studied the mechanism of the deposition process, the structure of the deposited SiOx films by various techniques and the role of a spinodal decomposition in controlling the distribution of oxidation states of silicon in the film. In general, most fabrication methodologies including MS and electrochemical etching of silicon provide a good control over the stoichiometry of compact films, but are not well-suited for simultaneously tailoring film porosity, nanostructure and stoichiometry. [13-28] These limitations have been overcome in the present work thanks to a new thin film synthesis procedure consisting of the room temperature reactive magnetron sputtering deposition (r-MS) at oblique angles (r-MS-OAD) that permits simultaneously tuning both film porosity and O/Si ratio. For electron beam evaporated OAD films, the dependence between nanocolumnar structure and deposition conditions has been amply discussed in literature [29, 30] and used for the fabrication of Si or SiO_x thin films with controlled nanocolumnar microstructure.[31, 32] However, except for an early publication of Nyberg et al. [20] and a very recent paper by us [18] no other works using r-MS have reported the possibility of controlling the chemical composition of oxide thin films by adjusting the deposition geometry during r-MS-OAD. Relying on the theoretical principles and ideas of these works, in the present paper we have used a parametric two-variables (i.e. oxygen partial pressure and deposition angle) approach to achieve a strict control over both O/Si ratio and nanostructure of the as-deposited SiO_x films.

The use of nanostructured SiO_x thin films for the fabrication of near infrared (NIR) optofluidic devices relies on their transparency in this spectral region and on the dependence of the absorption gap and refraction index (**n**) on their O/Si ratio [5, 9, 33, 34] with values of **n** at λ=1500 nm that vary from ~3.4/3.5 RIU for elemental silicon to ~1.4

RIU for SiO_2.[5] Adjusting the optical properties of compact SiO_x thin films by controlling their stoichiometry has been utilized for the fabrication of compact 1D-photonic structures that cannot be actuated by liquid infiltration (e.g., rugate optical filters, Bragg reflectors –BRs- or Bragg microcavities –BMs-). [35-38] The challenge in the present work is the fabrication of planar 1D-photonic structures consisting of porous/nanostructured SiO_x films prepared by magnetron sputtering that can be operated by liquid infiltration. With this purpose we have applied the r-MS-OAD methodology for the tailored fabrication of optofluidic-actuated 1D BRs and BMs, these latter for label-free transducer applications. The manufactured 1D-photonic structures have depicted a high reliability and sensitivity as refractive index liquid sensors. To our knowledge no similar attempt based on physical vapour deposition methods to manufacture NIR optofluidic sensor devices has been reported in literature. Furthermore, a clear advantage of the fabrication method is the fact that it proceeds at room temperature, thus enabling the direct integration of these optotofluidic structures onto sensitive substrates and demonstrating the possibility of directly integrating these NIR photonic transducers into micro- and nano-fluidic channels or onto the surface of optical fibres.

2. Experimental Section

2.1.- Fabrication of nanostructured SiO_x thin films and multilayers by reactive MS at oblique angles.

SiO_x thin films with controlled stoichiometry and nanostructure were prepared by reactive magnetron sputtering (r-MS) in an oblique angle deposition configuration (OAD). Series of thin films were fabricated by controlling both the oxygen partial pressure (or the oxygen flow rate) during deposition and the angle between substrate and target (α). In a previous work we proposed a parametric equation that, for a given deposition arrangement,

predictively obtained the stoichiometry of the SiO_x thin films as a function of these two parameters [18]. This formula reads as follows:

$$\frac{\chi_0}{\chi_\alpha} = 1 - \frac{\Xi}{exp^{\Xi} - 1}(1 - cos\alpha)$$

Where χ_0 and $\chi\alpha$ are the film stroichiometries in a normal (i.e., α=0) and in oblique angle configurations (i.e., at a given value of α) and **Ξ** the tehermallization degree of the sputtered atoms, depending on the distance between target and substrate and the mean free path of particles which, in turn, depends on the gas pressure in the deposition chamber. A fundamental assumption in this equation is that the surface arrival rate of sputtered silicon atoms changes with the deposition angle while that of oxygen molecules only depends on its partial pressure in the plasma gas.

A plot of different curves derived from this equation is presented in **Figure 1** where we have indicated the expected basic tendencies of nanostructure and porosity as a function of deposition angle (i.e., zones for compact, porous and well-defined nanocolumnar thin films). It is noteworthy, that this set of curves serves for the specific reactor utilized in the present work and that for other reactors new curves should be calculated using data accounting for their specific geometry and working conditions. Each curve corresponds to a series of samples characterized by a given stoichiometry but presenting quite different microstructures varying from compact and homogenous at α=0 to highly porous and nanocolumnar at high α values. In the present work we will show results for series of samples prepared along the curves for x= 0.4, 0.8, 1.2 and 1.6 plotted with dashed lines in the figure.

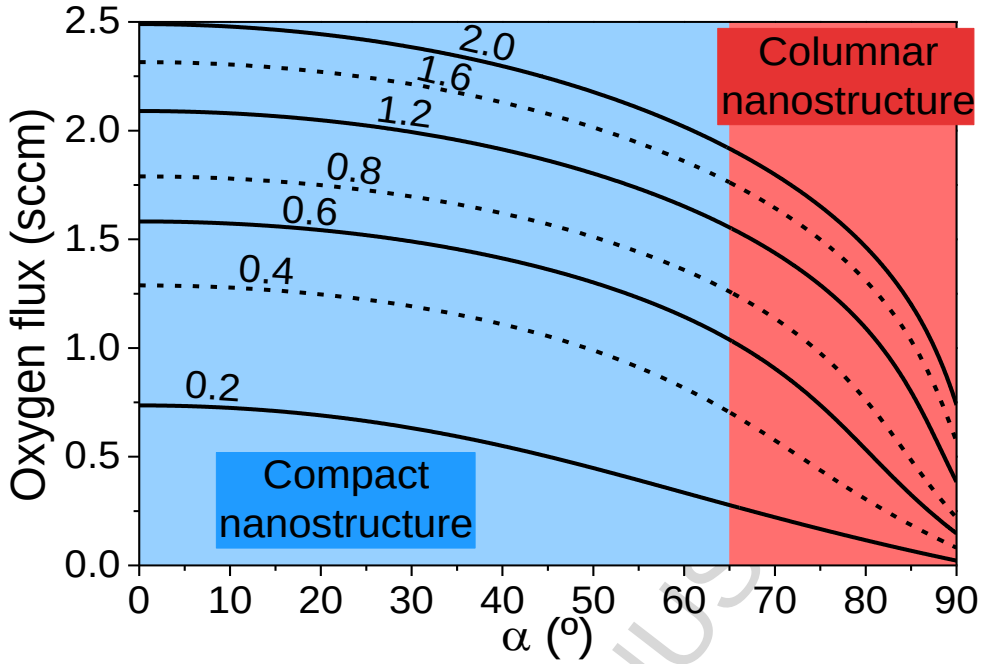

Figure 1.- Plot of iso-compositional curves of SiOx thin films prepared varying both oxygen flux and deposition angle for the experimental reactor utilized in the present work. These curves have been derived according to a parametric equation developed in ref. [18]

Samples were prepared by r-MS using a Si target (Gencoa Ltd, Liverpool, UK) and Ar as plasma gas (6.25 sscm or 0.15 Pa in our reactor) plus O_2 according to the flows in **Figure 1**. The magnetron was operated under pulsed DC regime at a frequency of 80 kHz, with a 2.5 ms off time and a constant electromagnetic power of 200 W. Samples were deposited on silicon, graphite and quartz substrates, depending on characterization tests. Samples are named by the nominal **x** value of a given series and, within a series, by the specific angle used for deposition (e.g., $SiO_{0.4}$-85º means a sample with a stoichiometric parameter **x** close to 0.4 that was prepared at an angle of 85° between target and substrate).

Multilayers formed by stacking SiO_x and SiO_2 films were prepared as 1D photonic systems in the form of BRs [39] or BMs [40] and were supported on quartz. Thickness of individual layers and their number were estimated by optical simulation. During the deposition of multilayers it was realized that the direct stacking of porous SiO_x and SiO_2 films may lead to a progressive loss of interface planarity and degradation of the microstructure, a structural effects which entailed undesired effects in terms of light dispersion and loss of interference pattern quality. This effect was apparent before liquid infiltration and could be counterbalanced by the deposition on top of the nanostructured SiO_2 films a thin (less than 20 nm) but homogeneous capping layer of the same material. As discussed in a previous publication, [41] this layer had little influence on the final optical properties of the photonic structure but contributed to preserve its microstructural integrity even when stacking a large number of layers. Capping layers were deposited as a continuation of the porous SiO_2 films by just changing the deposition angle from 85° to 0° and keeping constant all other parameters.

2.2.-Characterization of thin films and multilayers

Cross sectional and top view scanning electron microscopy (SEM) images were acquired with a field emission microscope (FESEM model Hitachi S4800 at the Instituto de Ciencia de Materiales de Sevilla, CSIC-US, Seville, Spain) for layers deposited on silicon substrates. These samples were conveniently diced for cross section analysis.

Focused ion beam SEM analysis of selected samples were carried out using a FEI Helios Nanolab 660 tool following a procedure previously reported. [42] A strip of Pt was deposited to prevent ion damage to the surface and ensuring conductivity. Subsequently, trenches were milled at 30 keV Ga^+ ion energy and the cuts observed with the electron beam under 52° incidence in the SE mode.

Rutherford Backscattering Spectrometry (RBS) of thin films was used to determine the O/Si ratio and the atomic thickness of films expressed in Si atoms/cm^2 [22, 23] in samples deposited on flat pyrolytic graphite. Experiments were carried out in a 3 MeV tandem accelerator at the Centro Nacional de Aceleradores (CNA, Seville, Spain) with a beam of 2.3 MeV alpha particles, accumulated doses about 10 mC, and 3 mm beam spot diameter, and a passivated implanted planar silicon (PIPS) detector located at 165° scattering angle. The RBS spectra were simulated with the SIMNRA software [43] The O to Si ratio defines the film stoichiometry and was obtained from the area of the bands of these two elements after calibration with the intensity ratio for a SiO_2 thin film measured under the same conditions.

Porosity, expressed in terms of percentage of void space in the SiO_x thin films, has been roughly determined by comparing their mass thickness (t_m) and their actual thickness (t_{SEM}) by means of the relation $\%V=[1-t_m/t_{SEM}]\cdot 100$. The actual thickness of the films t_{SEM} was determined by inspection of the cross section SEM micrographs of the samples. The mass thickness was approximated by the expression: $t_m = \left[\left(\frac{N}{N_A}\right) \cdot M_{SiO_x}\right] / \rho(SiO_x)$,where N is the number of SiO_x molecules obtained from the RBS measurements (assuming that each Si atom forms a SiO_x molecule), N_A the Avogadro's number, M_{SiOx} the molecular mass, and ρ_{SiO_x} the density of the silicon suboxide in bulk form. The density of the SiO_x thin films has been approximated according to $\rho_{SiO_x} = (1-x) \cdot \rho_{Si} + x \cdot \rho_{SiO_2}$, with ρ the density of the indicated compounds expressed in terms of grams per unit volume (g/cm^3).

X-ray photoelectron spectra (XPS) were recorded in the pass energy constant mode in a Phoibos 100 DLD (SPECS) spectrometer using the Mg Kα line as excitation source. The

binding energy (BE) scale of the spectra was referred to the C1s line at 284.5 eV of the adventitious carbon contaminating the surface of the samples. Fitting analysis of the Si 2p spectra has been carried out under the assumption that the different oxidation states of silicon, from Si^{4+} at 103.8 eV to Si^{0} at 99.6 eV, [7,13, 26, 44,45] have BEs varying by approximately one eV per unit of oxidation state. This approximation has been amply utilized in literature and, within a small margin of inaccuracy, has been demonstrated appropriate to characterize the different oxidation states of silicon in SiO_x materials. In the curse of the present investigation we found that just after a first exposure to air, the surface of SiO_x thin films became extra-oxidized to an extent that depended on their stoichiometry and porosity. This small surface oxidation by exposure to air stabilized the surface state which, for long periods of time, remained then unmodified. To prove the extent of surface oxidation, the XPS analysis of the thin films exposed to air was complemented with their analysis after sputtering with Argon ions (Ar^{+}) of 1000 eV up to a maximum time of 10 min and an etching rate of 0.2 nm min^{-1}, when no more changes could be detected in the spectra. This experiment proved that the oxidation layer was superficial (approximately 1-2 nm) and that the extra oxidation of the surface only corresponded to a change in x between 0.1-0.2 for most samples. However, since Ar^{+} ions may induce a preferential removal of oxygen from the SiO_x materials, assessment of surface stoichiometry will be done on the XPS spectra of non-sputtered samples. Average thin film stoichiometry will be referred to the RBS data.

2.3.-Optical and optofluidic analysis of nanostructured thin films and multilayers

UV-Vis-NIR transmission spectra in the range 200-2500 nm were recorded in a PerkinElmer spectrometer (UV/Vis/NIR Spectrometer Lambda 750S) for samples deposited on fused quartz substrates. Fitting analysis of these spectra to determine the

refraction index and thickness of the films was carried out according to the conventional approximation relying on a Cauchy dispersion of refractive index.

For pure and atomically homogenous compounds, absorption edges are typically determined using the so-called *Tauc Plot* [46] by representing $(Ahv)^n$(A, absorbance, and $n = {}^1/_2$ taken the SiO_x as an indirect bandgap semiconductor) against hv and then extrapolating to zero. Although we employed this method of evaluating absorption edges for the different SiOx samples, the obtained values will only be dealt with in a semiquantitative manner because the porous SiO_x films were heterogeneous in depth due to the extra oxidation of their outer layers.

Optofluidic analysis of SiO_x-SiO_2 multilayers was carried out in reflection geometry using an experimental device previously described in ref. [47], consisting of two optical fibers separated by 15º that were focused on the same spot of the layers. These optical fibers were used for excitation and recording the optical response of the photonic structures when they were infiltrated with liquids of different refraction indices $\mathbf{n}_{liq}$. Reflection was preferred to transmission because the investigated liquids present very intense bands in the NIR region that might overlap with the transmission gap features of the investigated photonic structures. This undesired effect is not observed in reflection because only the liquid infiltrated in the pores contributes to the spectrum and the absorption of this tiny volume is negligible (taken into account a porosity of 40%, a rough estimation renders a liquid volume of $4 \cdot 10^{-5}$ cm^3 for a photonic structure of 1micron thickness covering an area of $1cm^2$).

3. Results and Discussion

The development of NIR silicon photonics with 1D-nanocolumnar-SiO_x-SiO_2 multilayers as intended in this work entails the fabrication of nanostructured SiO_x thin films with well-defined optical properties and porosity. Therefore, in the first part of this work, we describe the synthesis by MS-OAD and the characterization by various techniques of these SiO_x thin films. Based on the obtained results, we will show that the dependence found between optical properties (i.e., $\mathbf{n_e}$ and absorption edge) and chemistry and nanostructure of the films provides a straightforward means for designing "a la carte" different types of 1D photonic structures suitable for optofluidic actuation.

3.1.-Synthesis and characterization of SiOx thin films by MS-OAD

The possibilities of the MS-OAD method developed in the present work for a tailored synthesis of nanostructured SiO_x thin films will be illustrated with results corresponding to four series of samples with nominal **x** values of 0.4, 0.8, 1.2 and 1.6 that were prepared at incident angles of 0º, 70º and 85º. Main characterization results are reported next.

3.1.1.-Chemistry of nanostructured SiOx thin films prepared by MS-OAD

The O/Si ratios for the four series of thin films deposited on graphite were determined by RBS (spectra are reported as supporting information **Figure S1**) and are gathered in **Table 1**. The reported values reveal that, for a given nominal stoichiometry, the actual O/Si ratio generally increased for the films prepared at 85º with respect to 0º, a feature that we attribute to some extra surface oxidation after air exposure.

Table 1.- O/Si ratios, porosity, refraction indices at 1500 nm, absorption edges and tilting angle of nanocolumns in the studied thin films. Porosity was calculated as explained in the experimental section.

	$SiO_{0.4}$			$SiO_{0.8}$			$SiO_{1.2}$			$SiO_{1.6}$			SiO_2 Ref.	
Deposition angle (°)	0	70	85	0	70	85	0	70	85	0	70	85	0	85
O/Si ratio (RBS) ±0.05	0.34	0.35	0.38	0.75	0.85	0.70	0.90	1.25	1.25	1.45	1.60	1.70	2.00	2.00
O/Si ratio (XPS) ±0.5	0.6	0.7	0.7	0.9	1.2	0.8	1.4	1.5	1.5	1.4	1.7	1.7	-	-
n (1500 nm) ±0.05	3.46	2.74	2.76	2.31	2.08	2.03	2.23	1.81	1.82	1.75	1.52	1.48	1.48	1.35
Absorption edge (eV) ±0.2	1.5	1.4	1.4	2.0	2.0	1.9	1.6	2.1	2.0	3.5	2.7	2.5	-	-
Porosity (%V)	15.2	37.1	43.0	15.1	39.1	38.9	19.4	35.3	42.6	17.3	39.1	40.0	-	33
Tilting angle columns (°)	0	43	47	0	35	42	0	33	34	0	31	28	0	29

Differences in film stoichiometry entailed different partitions in the chemical states of silicon as determined by XPS analysis. Si2p fitted spectra of samples $SiO_{0.4}$-0º/85º and $SiO_{1.6}$-0º/85º are presented in **Figure 2** (equivalent Si2p spectra of samples $SiO_{0.8}$-0º/85º and $SiO_{1.2}$-0º/85º samples are presented as **supporting information Figure S2)**. A first assessment of these spectra reveals that the partition of oxidation states is quite different for series $SiO_{0.4}$ and $SiO_{1.6}$, where, respectively, Si^{4+} or Si^0 species (at 103.8 and 99.6 eV BE [7, 13, 26, 44, 45]) are majority species. Differences in relative intensities can be also observed in the other fitting bands attributed to Si^{3+}, Si^{2+} and Si^{+} species. From the area of the fitting bands in the photoelectron spectra, we determined the relative concentration of each chemical state of silicon in the different samples (see supporting information **Table S2**). A common feature in all the samples is the low concentration of Si^{2+} species which is practically negligible in samples $Si_{0.4}$ and in sample $SiO_{1.6}$-85º. Minimization of Si^{2+} species in SiO_x samples prepared by physical vapour deposition has been previously attributed to an energetically favored dismutation into Si^{+} and Si^{3+} species. [13] The

situation is different in SiO_x prepared by thermal oxidation of silicon or presenting a spinodal decomposition where a different distribution of oxidation states can be found for a similar stoichiometry.[26, 44] The comparison of the O/Si ratios in Table 1 calculated by RBS or estimated from the areas of the Si2p and O1s XPS spectra show higher values in this latter case, in agreement with the superficial character of the XPS technique and the already mentioned surface oxidation of samples after air exposure.

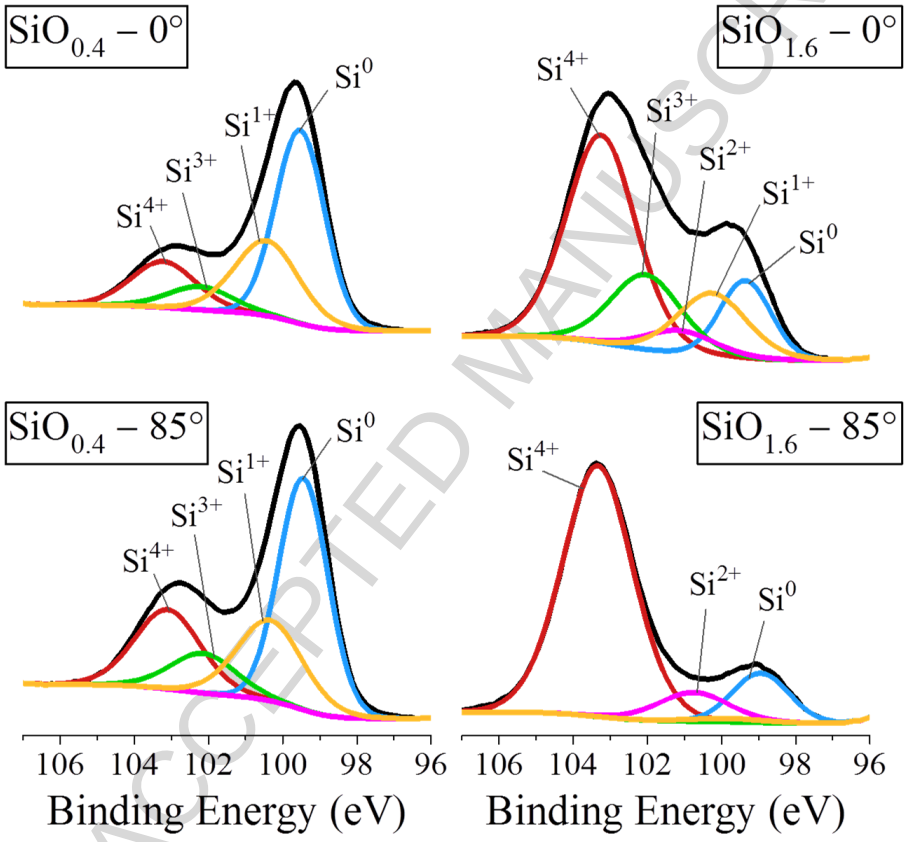

Figure 2.- Fitted spectra of selected samples of series $SiO_{0.4}$ and $SiO_{1.6}$

3.1.2.- Nanostructure and porosity of the SiOx thin films prepared by MS-OAD

The high porosity of SiO_x samples prepared at oblique deposition angles was confirmed by SEM analysis of the microstructure of the films. As examples, the cross section micrographs of samples series $SiO_{0.4}$ reported in **Figure 3** reveal a clear progression from a homogeneous and compact microstructure at normal deposition to a tilted nanocolumnar microstructure (tilting angles 45º and 48º) at oblique (i.e. 70º and 85º) deposition geometries. This behaviour agrees with the microstructure expected for thin films deposited at oblique angles where shadowing effects control the deposition process.[29, 48] A similar evolution was found for the other three series of investigated samples (see Table S2 and the SEM micrographs in supplementary information, **Figure S3**). An interesting effect observed for the series of investigated films is that the tilting angle of the nanocolumns (β) increased with the deposition angle (α) and for the films with the lowest O/Si ratio. This latter tendency agrees with that expected from the reported evolution of tilting angles of SiO_2 and elemental Si.[48]

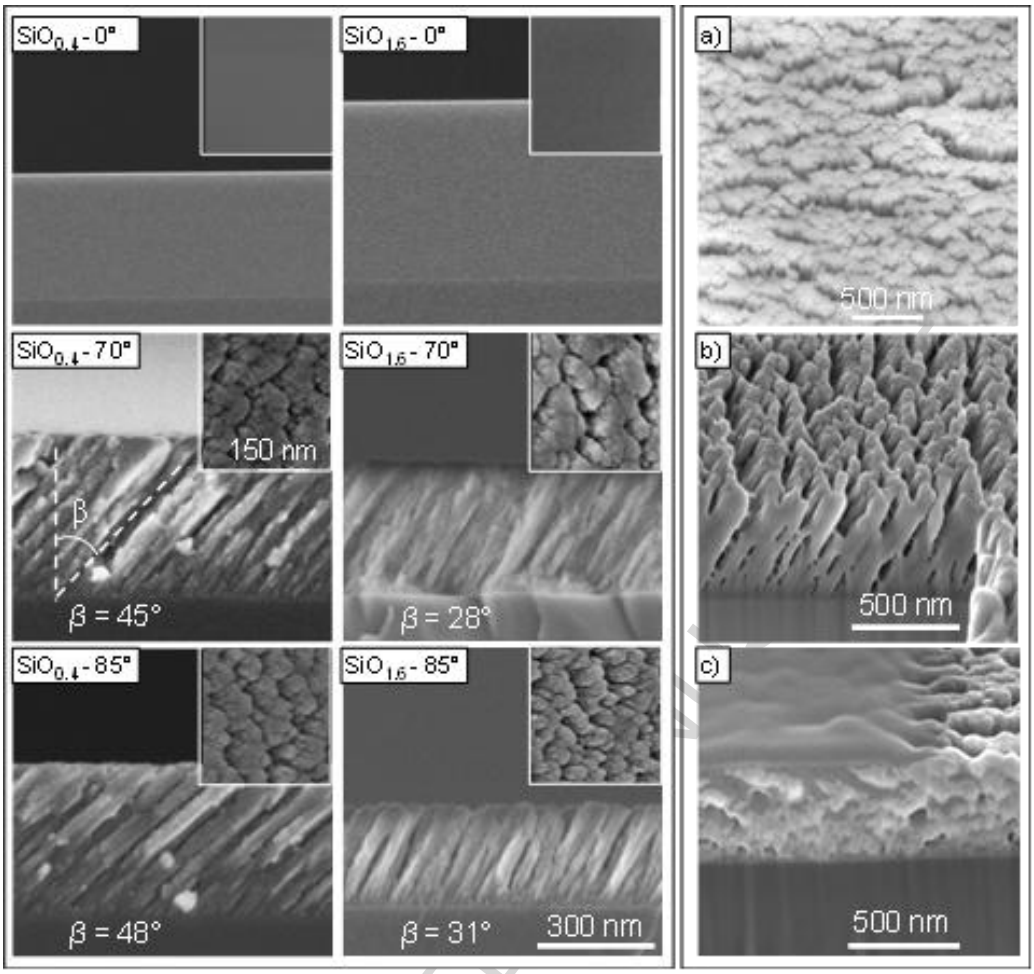

Figure 3.- Left) Cross section and normal (insets) SEM micrographs recorded for samples $SiO_{0.4}$ and $SiO_{1.6}$. Right) From top to bottom SEM micrographs taken in the FIB-SEM system for a SiO_2-85º film in normal view (a) and after cross sectioning along a direction perpendicular (b) and parallel (c) to the tilting direction of nanocolumns. The blurred zones in c) correspond to deposited platinum used to remove charging effects.

Pore structure of the films was directly assessed by FIB-SEM observation of cross sections along in-plane directions parallel and perpendicular to the incoming direction of sputtered atoms. The images in Figure 3 right) clearly confirm that the nanoculumns of these thin films leave free a considerable void space that goes from the surface to the bottom of the

films. Since all void space structure in these films is accessible to the exterior it will be filled in by liquid infiltration and eventually lead to the optofluidic modulation of their optical response.

The porosity of the films, estimated as reported in the experimental section, also varied with the deposition angles (c.f., **Table 1**) showing a progressive increase for the deposition at higher angles, a feature that agrees with the principles of the oblique angle deposition of thin films. 40% porosities are a good indication of the possibilities offered by SiO_x thin films prepared by MS-OAD for optofluidic photonic-device applications.

3.1.3.- Optical properties of SiOx thin films prepared by r-MS-OAD

Figure 4 shows the UV-Vis-NIR transmission spectra recorded for the four series of studied samples. According to these spectra, the SiO_x thin films were opaque in the UV and visible regions and present absorption edges that roughly increases with the O/Si ratio, in agreement with the evolution expected for a transition between elemental Si to SiO_2.[5] The values of band edges calculated according to the Tauc method [46] which are reported in **Table 1** confirms this tendency, except for small deviations for a given stoichiometry, suggesting that the samples are atomically heterogeneous and that the experimental band edge is defined by the domains with higher silicon content.

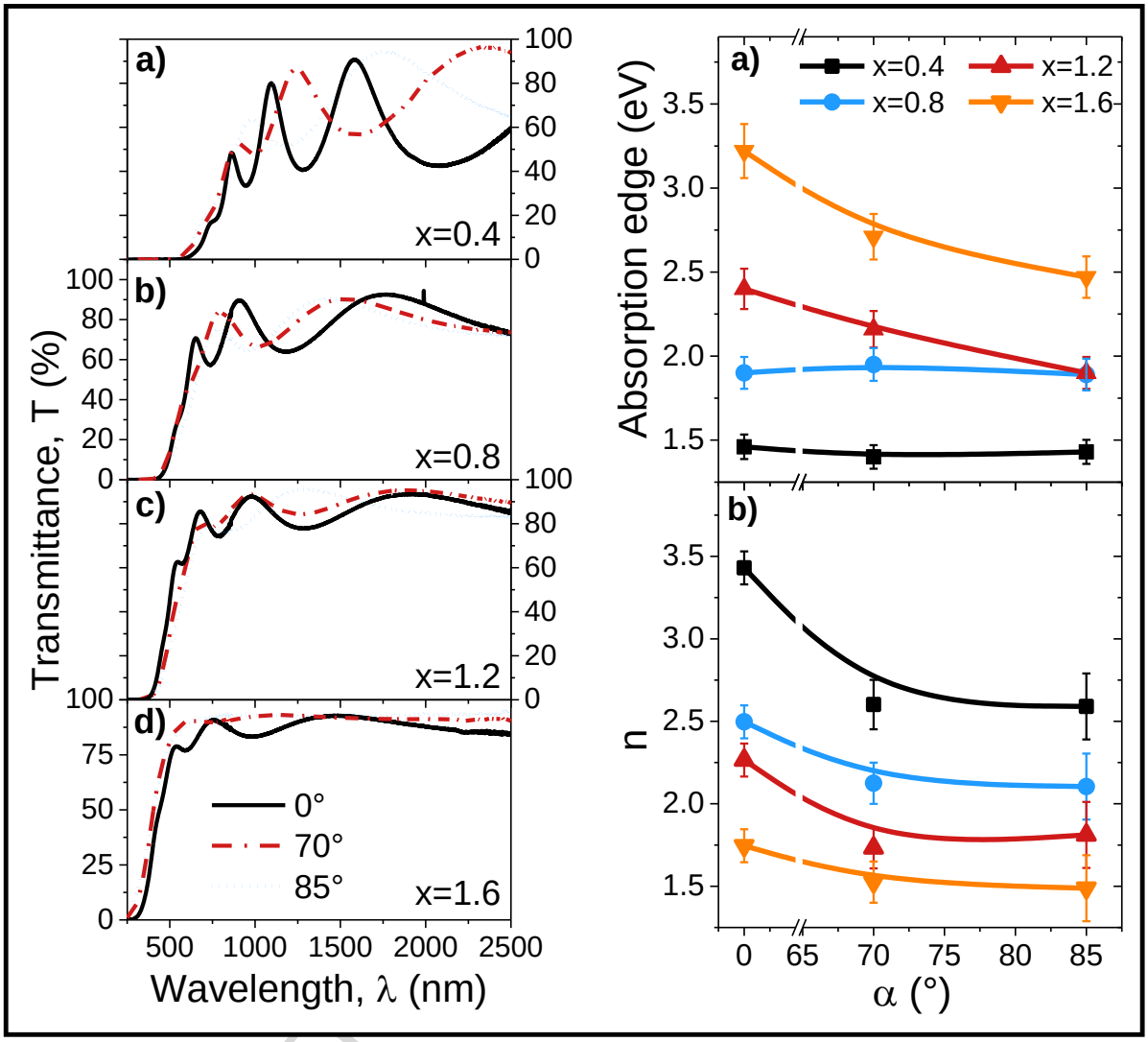

Figure 4.- Left) (a-d) UV-Vis-NIR transmission spectra of the four series of studied samples as a function of deposition angle as indicated. Right) (a) Absorption edges determined by the Tauc method (see experimental section) for the four series of SiO_x thin films. Calculated values are determined by the contribution of domains enriched in Si^0. (b) Refraction indexes as a function of deposition angle for the four series of SiO_x thin films.

From the viewpoint of the fabrication of photonic structures and their potential optofluidic applications, it is of the outmost importance to control the refraction index of the different films. From a Cauchy analysis of the curves in **Figure 4 left),** the refraction indices at λ=

1500 nm gathered in **Figure 4 right-b)** and Table 1were determined. The reported values show a net decrease from sample $SiO_{0.4}$ to $SiO_{1.6}$ that must be associated with the increase in oxygen content (a similar evolution was found for compact SiO_x thin films prepared by different methods [33, 34]) and, within each stoichiometric series, for the films prepared at oblique angles. According to the medium approximation theory [49] the refraction indices of porous SiO_x thin films must depend on the void space according to $\mathbf{n_e}$= f($\mathbf{n_s}$, $\mathbf{n_v}$), where $\mathbf{n_e}$ is the effective refraction index of the films, $\mathbf{n_s}$ that of the bulk SiO_x and $\mathbf{n_v}$ that of the air ($\mathbf{n_v}$=1) or condensates or liquids when they completely fill the pore space (i.e., in this case $\mathbf{n_v}$= $\mathbf{n_l}$).

3.2.- Development of NIR 1D-photonic structures for optofluidic and sensing applications.

Herein we want to illustrate how the possibility of tuning the optical properties of porous SiO_x thin films prepared by MS-OAD provides a straightforward means for the tailored synthesis of NIR 1D-photonic structures and their use for various optofluidic applications. These possibilities will be illustrated with some specific proof of concpet devices.

3.2.1.- NIR 1D-photonic structures made of SiOx thin films prepared by r-MS-OAD

Tuning the optical properties of porous SiO_x thin films provides a straightforward means for the tailored synthesis of NIR 1D-photonic structures. Stacking layers of two materials with a high contrast in refraction indices is a common way of fabricating 1D photonic structures [41, 50, 51]. A typical example consists of stacking TiO_2 and SiO_2 thin films which, in compact form, present refraction indices (at 550 nm) around 2.4 and 1.4 RIU, respectively. The NIR transparency of the SiO_x samples and the large difference in refraction index between SiO_2 and SiO_x (x<2) thin films (c.f., Figure 4) support the

feasibility of fabricating 1D photonic structures by stacking layers of silicon oxides prepared by the r-MS-OAD technique. Other authors have explored this possibility with compact SiO_x and SiO_2 stacked films [35-38], occasionally prepared by MS. Related self-standing silicon optical devices have been also prepared by electrochemical etching of silicon wafers to generate the so-called porous silicon.[52-54] However, these methods do not provide the flexibility and strict control of photonic properties of the herein developed physical vapour deposition procedure by which porosity and composition can be adjusted independently.

Porosity has been previously used to further control the photonic properties of one (e.g., ITO (indium tin oxide) [55] or two-materials multilayers. [40,41,50,51] Unlike other procedures of SiO_x thin film manufacturing,[5-9] the r-MS-OAD method offers the possibility of controlling both composition and porosity of the SiO_x thin films to tailor the optical properties of supported 1D-photonic structures. As example, four BRs have been prepared and tested in this work. They are formed by stacking eleven compact (BR-C) or porous SiO_x/SiO_2 (BR-P) alternant layers as defined in Table 1. Their reflectance spectra are presented in **Figure 5**.

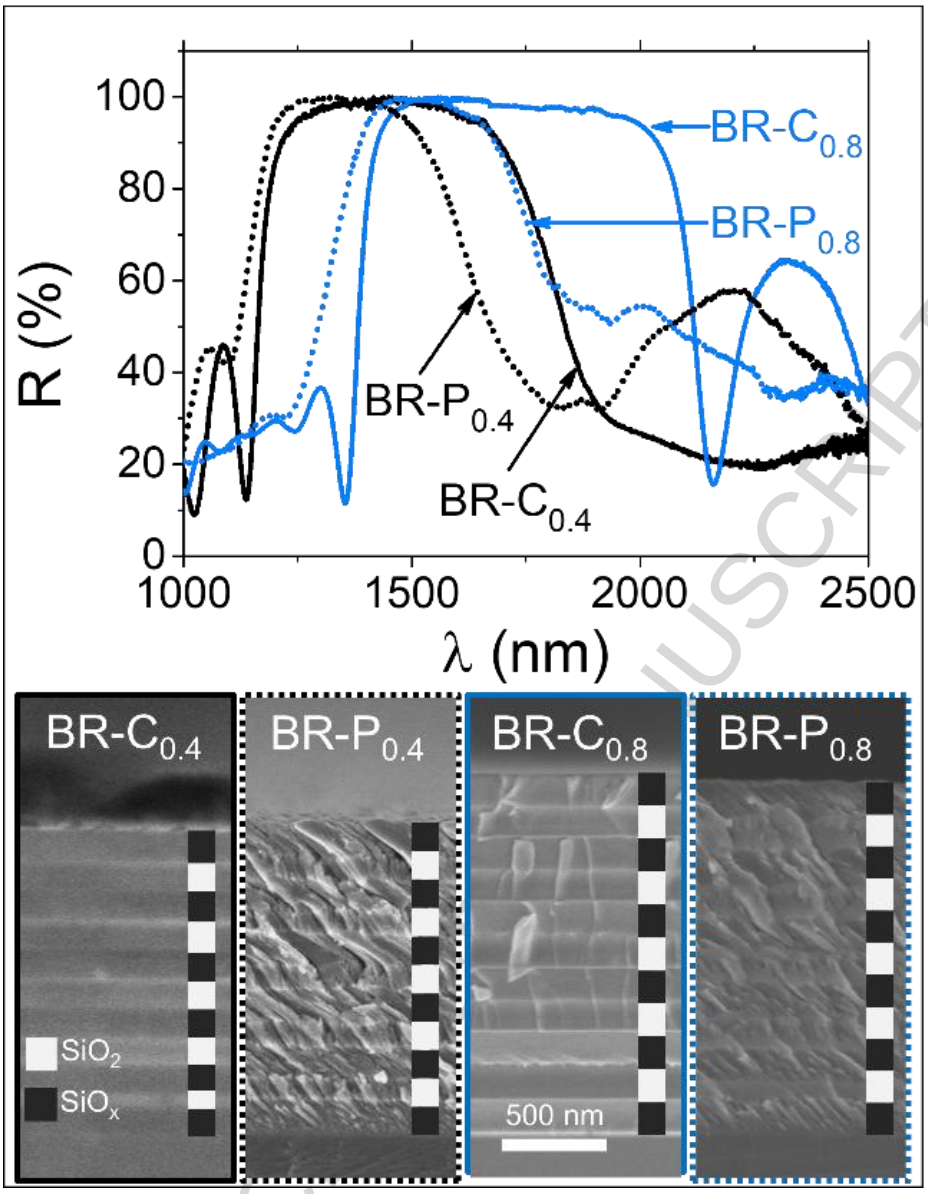

Figure 5.- Top) Series of normalized reflectance spectra recorded for compact and porous SiO_x/SiO_2 multilayers acting as BRs (see Table 1). Bottom) Cross section SEM micrograph of these multilayers, including a scheme of the stacking sequence of SiO_2 and SiO_x thin films.

The compact and porous/nanostructured character of the multilayers is clearly evidenced by the cross section SEM micrographs presented in Figure 5 bottom). Meanwhile, their spectra are characterized by a wide reflection band typical of this type of photonic structures. A

simple estimate of the optical behaviour of BRs is possible using the well-known formula:[56]

$$\frac{\Delta\lambda}{\lambda_0} = \frac{4}{\pi} asin \frac{n_H - n_L}{n_H + n_L} \qquad (1)$$

Where $\Delta\lambda$ is the reflection band width, λ_0 its central position and $\mathbf{n_H}$ and $\mathbf{n_L}$ the refraction indices of the high and low refraction index stacked materials, in our case SiO_x and SiO_2, respectively. The BRs reported in Figure 5 are made of $SiO_{0.4}/SiO_2$ and $SiO_{0.8}/SiO_2$ thin films of approximately 165/170 and 180/175 nm thickness, respectively.

According to Table 2, for the same SiO_X stoichiometry, band width must be much smaller for the porous BRs, in agreement with the smaller value of the $\mathbf{n_H}$-$\mathbf{n_L}$ difference in this case. In addition, the calculated $\Delta\lambda/\lambda_0$ values follow the tendencies determined experimentally, proving that optical properties of this type of structures can be tailored by adjusting not only the composition but also the porosity of the films. Additional examples of BRs prepared by r-MS-OAD varying the thickness of the individual layers or the stoichiometry of the porous SiO_x thin films are reported as supplementary information, Figure S4.

Table 2.- Description of the SiO_x/SiO_2 BRs whose reflection spectra are reported in Figure 5 and experimental and calculated $\Delta\lambda/\lambda_0$ values determined, respectively, from these spectra and from the refraction index values of the individual layers using formula (1).

BR	**Stacked films and thinckness (nm)**	**$nSiO_x$/ $nSiO_2$**	**$\Delta\lambda/\lambda_0$ (exp)/calc.)**
BR-$C_{0.4}$	$SiO_{0.4}/SiO_2$ - 0° (160)	3.43/1.45	0.43/0.52
BR-$P_{0.4}$	$SiO_{0.4}/SiO_2$ -85° (165)	2.59/1.38	0.36/0.39
BR-$C_{0.8}$	$SiO_{0.8}/SiO_2$ - 0° (180)	2.49/1.45	0.41/0.35
BR-$P_{0.8}$	$SiO_{0.8}/SiO_2$ -85° (175)	2.10/1.38	0.31/0.27

3.2.2.-Optofluidic properties of SiO_x-SiO_2 NIR Bragg mirrors

The high porosity of the SiO_x-SiO_2 BRs permits to fine tuning their optical properties by optofluidic modulation. In the visible wavelength region, we have previously studied the optofluidic modulation of optical properties of TiO_2-SiO_2 porous multilayers in the shape of 1D-photonic crystal (or likewise BR) prepared by electron beam evaporation at oblique angle.[42, 50] At a preliminary level, similar effects upon condensation of vapours have been studied in self-standing porous silicon distributed Bragg reflectors prepared by electrochemical etching.[1-4, 52-54],

An analysis of the possibilities of the liquid infiltration technique to modify the NIR optical properties of the BMs prepared by r- MS-OAD is reported in **Figure 6**. This figure shows the reflectance spectrum of a BM formed by eleven $SiO_{0.4}$-85º and SiO_2-85º thin films (approximate thickness 180nm, see Figure 6 (bottom)) in its original form (i.e with its pores filled with air) and infiltrated with liquids of different refraction indices varying from 1.3 (water) to 1.74 (diiodomethane). The spectra reveal that filling the pores of the SiO_x and SiO_2 nanocolumnar thin films produces a widening of the Bragg gap and a redshift towards longer wavelengths. These effects must be attributed to the increase in the $\mathbf{n_e}$ values of the single layers of the stack because of the substitution of the air filling the pores by the different liquids (i.e., according to $\mathbf{n_e}=f(\mathbf{n_s}, \mathbf{n_l})$. The observed optical changes were reversible and their magnitude could be fine controlled by adjusting the refraction index of the infiltration liquid (e.g., using mixtures of liquids or solutions of controlled concentrations). In the experiments reported in Figure 6 a maximum widening by approximately 60 nm and a redshift displacement by 30 nm was found when comparing the original spectrum and the one recorded after diiodomethane infiltration. Thanks to the scalability of the r-MS-OAD technique and its compatibility with any kind of substrate, it is

believed that liquid modulation of optical properties of BRs prepared by this method can be of much interest for energy and other related applications requiring a fine tuning of the reflectivity of selective mirrors [57].

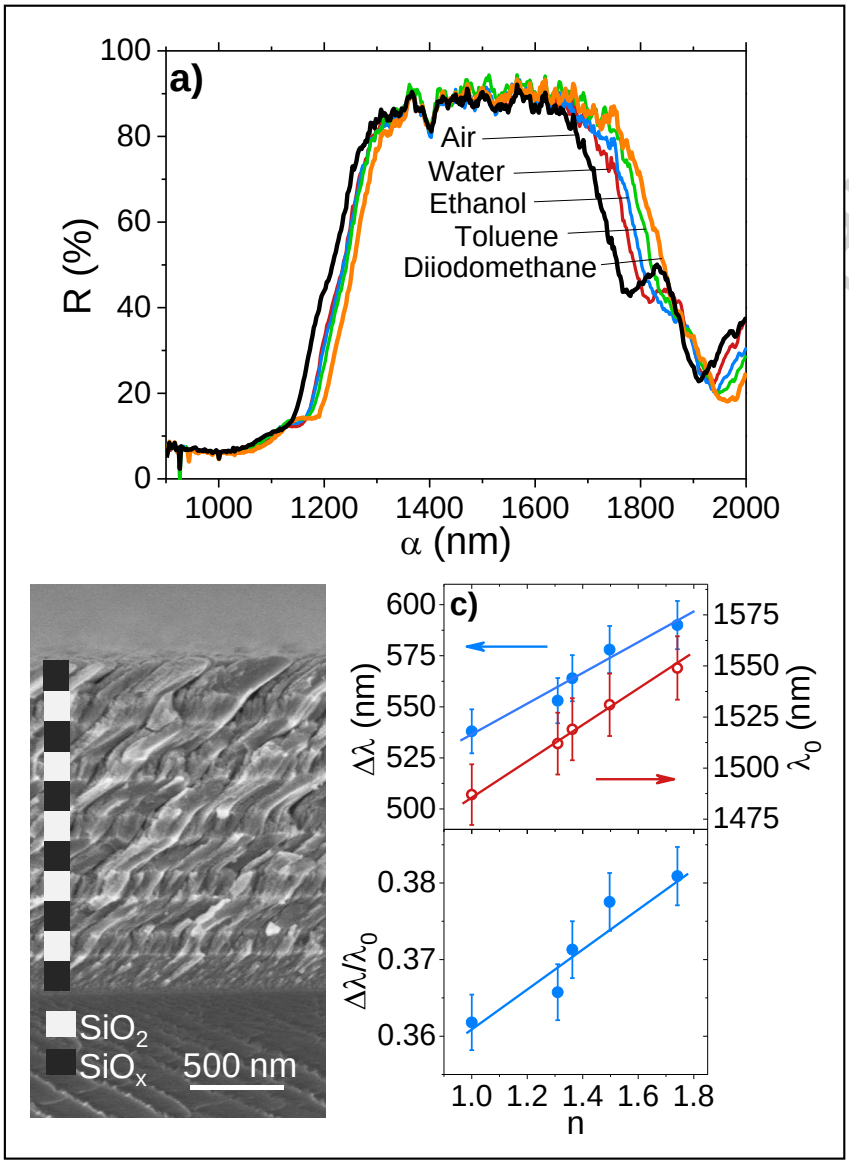

Figure 6.- a) Normalized reflection spectra of a BR made by the stacking of eleven $SiO_{0.4}/SiO_2$-85º thin films with an approximate thickness of 180nm, as prepared and after infiltration with liquids of increasingly higher refraction indices. b) SEM cross section

micrograph. c) representation of $\Delta\lambda$, λ_0 and $\Delta\lambda/\lambda_0$ as a function of the refraction index of the liquid infiltrating the BR.

3.2.3.-NIR label free sensing devices based on SiO_x-SiO_2 Bragg microcavities

Porous BMs have been previously used for label-free refractive index sensor applications, generally in self-supported form. [4, 42, 52, 53] The new concept proposed here entails the modulation of optical properties in the NIR spectral region of BMs in the form of a supported film made by the stacking of SiO_x and SiO_2 porous layers prepared by r-MS-OAD. The cross section SEM micrograph reported in **Figure 7 c)** shows that this BM integrates two BRs made of five stacked $SiO_{0.8}/SiO_2$ nanocolumnar layers separated by a thicker SiO_2 layer acting as optical defect. All the films were prepared by r-MS-OAD at 85° and had an internal porosity of the order of 40%. The presence of a thicker layer acting as optical defect gives rise to a resonant peak in the reflection band that can be used for better following the optofluidic response of the system upon liquid infiltration. For a first set of experiments intended to prove that the BM optical properties change with the refraction index of the liquid infiltrated in its pores, Figure 7a) shows the reflection spectra recorded for this porous $SiO_{0.8}$-85º/SiO_2-85º BM infiltrated with liquids of different refraction indices varying from 1.3 to 1.7, approximately. The inset in Figure 7a) shows an enlarge plot of the resonant peak spectral zone to clearly visualize the magnitude of the peak shift depending on the refraction index of the infiltrated liquid. Meanwhile, the plot in Figure 7 b) reveals that the magnitude of the shift in the resonant peak position directly correlates with the refraction index of the liquid infiltrating the BM. Assuming that this correlation follows a lineal relationship, it is possible to estimate that the sensitivity for detecting changes in the refraction index of liquids following the redshift of the resonant

peak of this device is approximately 90.4 nm RIU^{-1}. The feasibility of using this photonic device as label free refractive index sensor to analyse mixtures of liquids or solutions in a continuous mode (i.e. implementable in microfluidic devices) is further demonstrated in Figure 7 d)-e) showing the evolution of the difference spectra in the zone of the resonant peak when continuously monitoring a mixture formed by the addition of hexane to toluene. Similar results were obtained using other liquid mixtures of aqueous solutions of increasing concentration. These difference spectra reflect the effect of a little but progressive red shift in the position of the resonant peak and provide a much more sensitive procedure to determine the refraction index of liquid mixtures or solutions. The series of dots in Figure 7 e) corresponds to the values of ΔR_{max}-ΔR_{min} for mixtures with increasing molar fractions of toluene. Interestingly, these points can be adjusted with a straight line reproducing the expected refraction indexes of the liquid mixtures taken as the average of the contribution of the two components and assuming that there is no volume contraction in the mixture. From the slope of this line, the sensitivity achieved using this measurement procedure can be estimated as 219.9 R(%) RIU^{-1}, which compares well with that reported for TiO_2-SiO_2 optofluidic BMs operating in the visible,[47] or for electrochemically etched 3D porous self-supported silicon membranes. [4, 54] A limit of detecting refraction index changes of approximately 0.002 RIU can be deduced from these experiments. Clearly, this optofluidic analysis of pure liquids or mixtures of liquids supports the use of the SiO_x BMs in the form of thin films and prepared by MS-OAD for the label-free quantitative analysis of small volumes of binary mixtures of liquids or solutions. Progression regarding the detection of specific molecules are expected by anchoring specific molecules to the internal surfaces of the multilayer in a similar way than with porous silicon devices intended for biomolecule detection. [1-3]

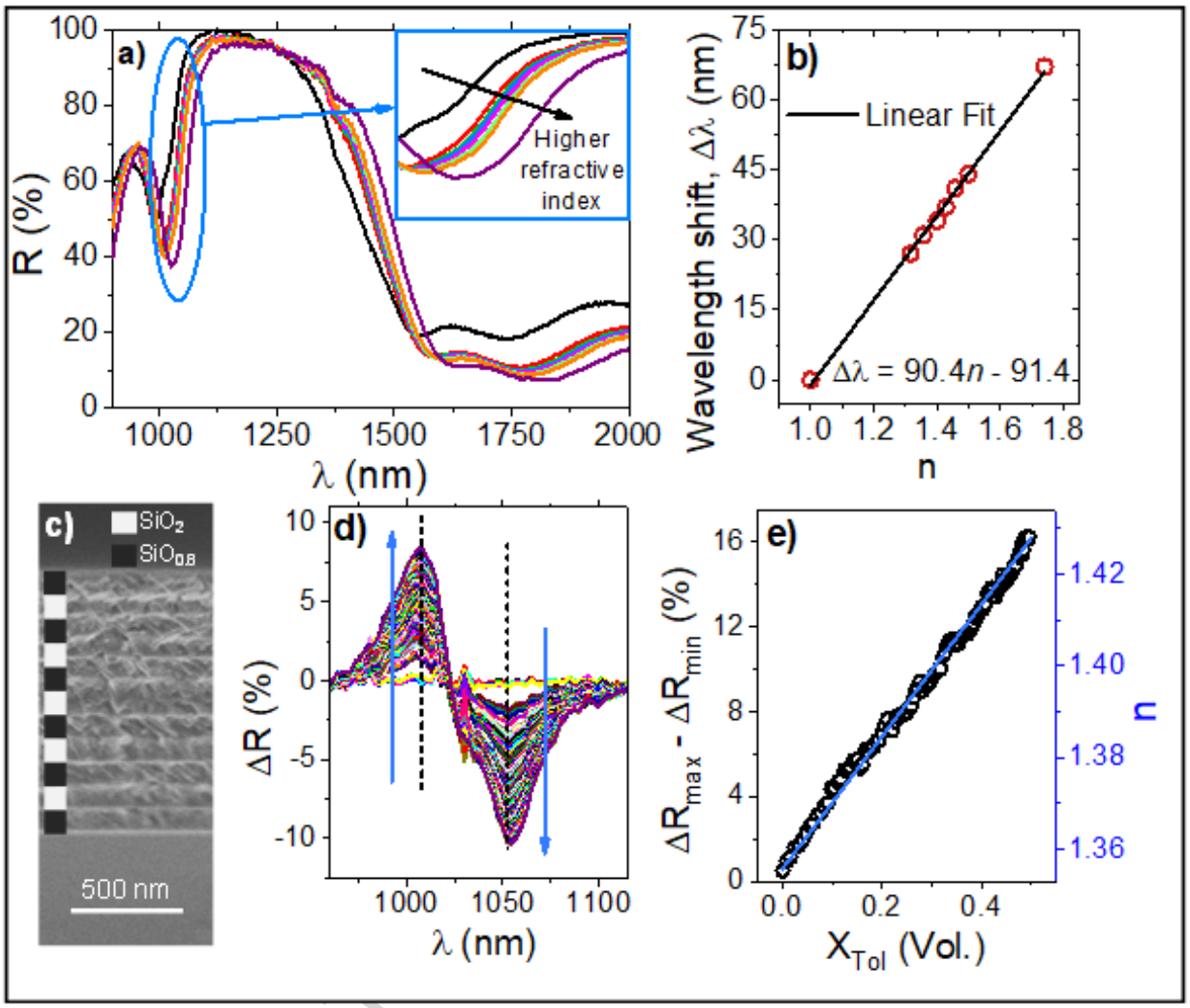

Figure 7.- a) normalized NIR spectra recorded for a poroous BM prepared by r-MS-OAD and infiltrated with liquids of different refraction indices (see text). The inset shows an enlargement of the resonant peak zone to better appreciate the magnitude of the redshift. b) plot of the resonant peak position as a function of the refraction index of the liquid infiltrated in the BM. Data points correspond to water (n=1.31), hexane (n=1.35), octane (n=1.40), cyclohexane (n=1.43), cyclooctane (n=1.46), toluene (n=1.50) and diiodomethane (n=1.70). c) SEM cross section micrograph and scheme of the SiO_2/SiO_x stacking. d) Difference spectra at the resonant peak spectral zone when the BM is infiltrated with toluene/hexane mixtures for increasing molar ratio of the former. e) Plot of the maximum minus minimum reflectance in the difference spectra in c) as a function of the toluene

molar ratio. The calculated refraction index of these mixtures, considering that there are no volume contraction effects, is superimposed in the plot.

On the other hand, the use of these thin film BMs is advantageous because of their compatibility with NIR optical components currently utilized for the analysis of liquids or their manipulation [58-61] and very common in a large series of optical devices such as absorbing materials and night vision LCD monitors. [62] In comparison with typical porous silicon devices used for label free sensing of liquids and biomolecules,[1-3] gas sensors [52, 53] or laser tunable [63] applications, a remarkable difference of the herein developed photonic structures is their thin film character and the fact that they can be prepared in one step on any kind of substrate, including polymers. This feature and its capacity for direct integration into micro- or even nano-microfluidic devices [64, 65] (a rough estimation of liquid volume required to fill the pore volume of the BM renders a liquid volume of $4 \cdot 10^{-5}$ cm^3 for a photonic structure of 1micron thickness covering an area of $1cm^2$) or at the tip of suitable optical fibres are additional advantages of this kind of optofluidic 1D-photonic structures made of SiO_x thin films prepared by MS. In this work, we have demonstrated that this technique, developed more than a decade ago for the preparation of SiO_x thin films in compact form [18-26], can be efficiently modified when working in an oblique angle configuration to control both stoichiometry and porosity of SiO_x thin films. The possibilities of this new approach have been demonstrated for the fabrication of complex photonic structures which successfully compete with classical electrochemical methods [1-4, 52-54] for the fabrication of label free sensor devices.

4. Conclusion

In this work, we have demonstrated the possibility of controlling the composition in nanostructured SiO_x thin films prepared by MS in an oblique angle configuration. We have proved that this method permits a strict and simultaneous control over the stoichiometry and nanostructure of the films. Following the predictions of a parametric formula, different sets of SiO_x thin film samples, with compositions varying from $SiO_{0.4}$ to $SiO_{1.6}$ and different microstructures from compact to nanocolumnar, have been prepared as a function of the oxygen flow and deposition angle during their MS deposition. The different characteristics of the layers, including composition, microstructure and atomic structure, have been thoroughly studied by XPS and SEM. In addition, the UV-Vis-NIR characterization analysis of their optical properties has evidenced the possibilities of the synthesis method to prepare nanostructured thin films with optical properties defined "a la carte".

Regarding the development of NIR 1D photonic structures, we have also shown that control over porosity provides an additional means to separately adjust refraction index and absorption edge, thus outperforming the functionality of compact SiO_x thin films prepared by conventional MS or other classical methods. In particular, we have shown that the SiO_2 and SiO_x thin films may display quite different **n** values and that this provides much flexibility for the manufacturing of photonic multilayers made by the successive stacking of SiO_x and SiO_2 thin films. Another outstanding feature of this type of NIR photonic structures is that they may be prepared using silicon as unique target material (i.e., just varying the amount of oxygen in the stacked layers) and that they can be prepared in a single step by MS. The reproducibility of the method in other reactors through the use of the proposed parameterized equation and its relatively easiness for up-scaling are additional

advantages of the proposed r-MS-OAD methodology for the fabrication of SiO_x thin films or more complex multilayer structures.

The flexibility and robustness of the developed r-MS-OAD method have resulted very useful for the manufacturing of optofluidic photonic devices. We have firstly shown that control over porosity and composition offers additional possibilities to control band widths and central positions of BRs even if the thickness of the individual stacked layers does not differ significantly. We have also shown that the porous character of the multilayers makes them suitable for optofluidic applications. Firstly, we have shown that the optical response in the NIR (position and gap width) of BMs changes systematically with the refraction index of the liquids infiltrated in the void space of the multilayer structure. Similarly, experiments with BMs have shown that this type of devices can be used for the development of liquid sensors working in the NIR spectral region. Additional applications can be forecast combining the tuning capacity of the optical properties of thin films and multilayers and their modification by liquid infiltration.

Acknowledgements

The authors thank the European Regional Development Funds program (EU-FEDER) and the MINECO-AEI (201560E055 and MAT2016-79866-R and network MAT2015-69035-REDC) for financial support. We also acknowledge the support of the University of Seville (V and VI PPIT-US).

References

[1] V. S.-Y. Lin, K. Motesharei, K.-P. S. Dancil, M. J. Sailor, M. R. Ghadiri. A porous silicon-based optical interferometric biosensor. *Science* 278 (1997) 840-843.

[2] S. Mariani, L. M. Strambini, G. Barillaro. Femtomole Detection of Proteins Using a Label-Free Nanostructured Porous Silicon Interferometer for Perspective Ultrasensitive Biosensing. *Anal. Chem.* **2016**, 88, 8502-8509.

[3] S. Mariani, L. Pino, L. M. Strambini, L. Tedeschi, G. Barillaro. 10 000-Fold Improvement in Protein Detection Using Nanostructured Porous Silicon Interferometric Aptasensors *ACS Sensors*, 2016, 1, 1471-1479.

[4] R. Caroselli, D. Martín-Sanchez, S. Ponce Alcántara; F. Prats Quilez, L. Torrijos Morán; J. García-Ruperez, Real-Time and In-Flow Sensing Using a High Sensitivity Porous Silicon Microcavity-Based Sensor. *Sensors* 17 (**2017)** 2813 1-12.

[5] N. Tomozeiu, N. Silicon Oxide (SiOx, 0<x<2): a Challenging Material for Optoelectronics. Optoelectronics - Materials and Techniques, P. Predeep [Ed.], InTech, DOI: 10.5772/20156. **2011;**

[6] D.Y. Qu, X.H. You, X.K. Feng, J. Wu, D. Liu, D. Zheng, Z.Z. Xie, D.Y. Qu, J.S. Li, H.L. Tang. Lithium ion supercapacitor composed by Si-based anode and hierarchal porous carbon cathode with super long cycle life. Appl. Surf. Sci. 463 (2019) 879-888

[7] A. Barranco, F. Yubero, J.P. Espinós, P. Groening, A.R. González-Elipe, Electronic state characterization of SiOx thin films prepared by evaporation, J. Appl. Physics 97 (2005) 1-5.

[8] D. Das, P. Mondal. Effect of oxygen on the optical, electrical and structural properties of mixed-phase boron doped nanocrystalline silicon oxide thin films. Appl. Surf. Sci. 423 (2017) 1161-1168

[9] D.E. Vázquez Valerdi, J.A. Luna López, G. García Salgado, A. Benítez Lara, J. Carrillo López, N.D. Espinosa Torres, Twofold SiO_x films deposited by HFCVD: Its optical, compositional and electrical properties, Proc. Eng. 87 (2014) 168-171.

[10] H. Liu, Y.J. Zou, L.Y. Huang, H. Yin, C.Q. Xi, X. Chen, H.W. Shentu, C. Li, J.J. Zhang, C.J. Lv, M.Q. Fan. Enhanced electrochemical performance of sandwich-structured polyaniline-wrapped silicon oxide/carbon nanotubes for lithium-ion batteries. Appl. Surf. Sci. 442 (2018) 2014-212

[11] T. Chen, J. Wu, Q. Zhang, X. Su. Recent advancement of SiOx based anodes for lithium-ion batteries. J. Power Sour. 363 (2017) 126-144.

[12] C. Liu, K. Qian, D.N. Lei, B.H. Li, F.Y. Kang, Y.B. He. Deterioration mechanism of LiNi0.8Co0.15Al0.05O2/graphite-SiOx power batteries under high temperature and discharge cycling conditions. J. Mater. Chem. A 6 (2018) 65-72.

[13] A. Barranco, J.A. Mejías, J.P. Espinós, A. Caballero, A.R. González-Elipe, F. Yubero, Chemical stability of Si^{n+} species in SiOx (x<2) thin films, J. Vac. Sci. Technol. A. 19 (2001) 136-144.

[14] M. Martyniuk, C.A. Musca, J.M. Dell, L. Faraone, Long-term environmental stability of residual stress of SiNx, SiOx, and Ge thin films prepared at low temperatures, Mater. Sci. Eng. B. Adv. Funct. Sol. Stat. Mater. 163 (2009) 26-30.

[15] H. T. Liu, Z.H. Huang, J.T. Huang, M.H. Fang, Y.G. Liu, X.W. Wu. Thermal evaporation synthesis of SiC/SiOx nanochain heterojunctions and their photoluminescence properties. J. Mater. Chem. C 2 (2014) 7761-7767

[16] S.Mukhopadhyay, S. Ray. Silicon rich silicon oxide films deposited by radio frequency plasma enhanced chemical vapor deposition method: Optical and structural properties. Appl. Surf. Sci. 257 (2011) 9717-9723

[17] F. Boke, I. Giner, A. Keller, G. Grundmeier, H. Fischer. Plasma-Enhanced Chemical Vapor Deposition [PE-CVD] yields better hydrolytical stability of biocompatible SiOx thin films on implant alumina ceramics compared to rapid thermal evaporation Physical Vapor Deposition (PVD). ACS Appl. Mater. Interf. 8 (2016) 17805-17816.

[18] A. García-Valenzuela, R. Alvarez, M.C. López-Santos, F.J. Ferrer, V. Rico, E. Guillen, M. Alcon-Camas, R. Escobar-Galindo, A.R. González-Elipe. A. Palmero. Stoichiometric control of SiOx thin films grown by reactive magnetrón sputtering at oblique angles. Plasma Proc. Polym. 13 (2016) 1242-1248.

[19] F. Huang, Q.M. Song, M. Li, B. Xie, H.Q. Wang, Y.S. Jiang, Y.Z. Song. Influences of annealing temperature on the optical properties of SiOx thin film prepared by reactive magnetron sputtering. Appl. Surf. Sci. 255 (2008) 2006-2011.

[20] T. Nyberg, C. Nender, H. Hogberg, S. Berg. The influence of the deposition angle on the composition of reactively sputtered thin films, Surf. Coat. Technol. 242 (1997) 94-95.

[21] N. Tomozeiu, E.E. van Faassen, W.M. Arnoldbik, A.M. Vredenberg, F.H.P.M. Habraken. Structure of sputtered silicon suboxide single- and multi-layers. Thin Sol. Films 420 –421 (2002) 382–385.

[22] E.D. van Hattum, A. Palmero, W.M. Arnoldbik, F.H.P.M. Habraken. Experimental characterization of the deposition of silicon suboxide films in a radiofrequency magnetron reactive sputtering system. Surf. Coat. Technol. 188–189 (2004) 399– 403.

[23] E.D. van Hattum, W.M. Arnoldbik, A. Palmero, F.H.P.M. Habraken. On-line characterisation of radiofrequency magnetron sputter deposition of SiOx using elastic recoil detection. Thin Sol. Films 494 (2006) 13 – 17.

[24] E. D. van Hattum, A. Palmero, W. M. Arnoldbik, H. Rudolph, F. H. P. M. Habraken. Distinct processes in radio-frequency reactive magnetron plasma sputter deposition of silicon suboxide films. J. Appl. Phys. 102 (2007) 124505 1-11.

[25] E.D. van Hattum 1, D.B. Boltje, A. Palmero 2, W.M. Arnoldbik, H. Rudolph *, F.H.P.M. Habraken. On the argon and oxygen incorporation into SiOx through ion implantation during reactive plasma magnetron sputter deposition. Appl. Surf. Science 255 (2008) 3079–3084

[26] J. J. van Hapert, A. M. Vredenberg, E. E. van Faassen, N. Tomozeiu, W. M. Arnoldbik, and F. H. P. M. Habraken. Role of spinodal decomposition in the structure of SiOx. Phys. Rev. B 69 (2004) 245202 1-8.

[27] J. Alvarez, P. Bettotti, I. Suarez, N. Kumar, D. Hill, V. Chirvony, L. Pavesi, J. Martínez-Pastor. Birefringent porous silicon membranes for optical sensing, Opt. Express 19 (2011) 2610626116.

[28] T. Jalkanen, V. Torres-Costa, J. Salonen, M. Björkqvist, E. Mäkilä, J.M. Martínez-Duart, V-P Lehto, Optical gas sensing properties of thermally hydrocarbonized porous silicon Bragg reflectros, Opt. Express 17 (2009) 5446-5456.

[29] A. Barranco, A. Borras, A.R. Gonzalez-Elipe, A. Palmero, Perspectives on oblique angle deposition of thin films: From fundamentals to devices, Progr. Mater. Sci. 76 (2016) 59-153.

[30] R. Alvarez, J.M. Garcia-Martin, M.C. Lopez-Santos, V. Rico, F.J. Ferrer, J. Cotrino, A.R. González-Elipe, A. Palmero. On the Deposition Rates of Magnetron Sputtered Thin Films at Oblique Angles. Plasma Proc. Polym. 11 (2014) 571-576.

[31] M.D. Fleischauer, J. Li, M.J. Brett, Columnar Thin Films for Three Dimensional Microbatteries. *J. Electrochem. Soc*. 156 (**2009)**, A33-A36.

[32] P.R. Abel, Y.M. Lin, H. Celio, A. Heller, C.B. Mullins. Improving the Stability of Nanostructured Silicon Thin Film Lithium-Ion Battery Anodes through Their Controlled Oxidation. ACS Nano 6 (2012) 2506-2516.

[33] P.P. Dey, A. Khare, Stoichiometry-dependent linear and nonlinear optical properties of PLD SiOx thin films, J. Alloy Compounds 706 (2017) 370-376.

[34] S. Ilday, G. Nogay, R. Turan, Spectroscopic ellipsometry study of Si nanocrystals embedded in a SiOx matrix: Modelling and optical characterization, Appl. Surf. Science 318 (2014) 256-261.

[35] Q. Song, F. Huang, M. Li, B. Xie, H. Wang, Y. Jiang, Y. Song, Graded refractive-index SiOx infrared filters by reactive magnetron sputtering, J. Vac. Sci. Technol. 26 (2008) 265-269.

[36] H. Yoda, K. Muro, K. Shiraishi, Fabrication of rugate optical filters using a-SiOx:H Thin films, IEICE Trans. Electron. E91 (2008) 1639-1643.

[37] S.Y. Turishchev, V.A. Terekhov, D.A. Koyuda, A.V. Ershov, A.I. Mashin, E.V. Parinova, D.N. Nesterov, D.A. Grachev, I.A. Karabanova, E.P. Domashevskaya, Formation of silicon nanocrystals in multilayer nanoperiodic a-SiOx/insulator structures from the results of synchrotron investigations, Semiconductors 51 (2017) 349-352.

[38] J. Alarcon-Salazar, I.E. Zaldivar-Huerta, M. Aceves-Mijares, Electrical and electroluminescent characterization of nanometric multilayers of SiO_X/SiO_Y obtained by LPCVD including non-normal emission, J. Appl. Phys. 119 (2016) 215101 1-8.

[39] L. González-García, G. Lozano, A. Barranco, H. Miguez, A.R. González-Elipe, TiO_2–SiO_2 one-dimensional photonic crystals of controlled porosity by glancing angle physical vapour deposition, J. Mater. Chem. 20 (2010) 6408-6412.

[40] L. Tong, W. Qi , M. Wang, R. Huang , R. Su, Z. He. Tunable Design of Structural Colors Produced by Pseudo-1D Photonic Crystals of Graphene Oxide. Small 12 (2016) 3433-3443.

[41] A. García-Valenzuela, C. López-Santos, R. Alvarez, V. Rico, J. Cotrino, A.R. González-Elipe, A. Palmero, Structural control in porous/compact multilayer systems grown by magnetron sputtering, Nanotechnology 19 (2017) 465605 1-9.

[42] M. Oliva-Ramírez, A. Barranco, M. Löffler, F. Yubero, A.R. González-Elipe, Optofluidic Modulation of self-associated nanstructural units forming planar Bragg microcavities ACS Nano 10 (2016) 1256-1264.

[43] Mayer M, SMNRA User´s Guide, Tech. Rep. IPP 9/113, Max-Plank Institut für Plasmaphysik, Garching, Germany 1997.

[44] F.J. Himpsel, F.R. McFeely, A. Taleb-Ibrahimi, J.A. Yarmoff, G. Hollinger, Microscopic structure of the SiO2/Si interface, Phys. Rev. B 38 (1988) 6084-6096.

[45] N. Koshizaki, U. Umehara, T. Oyama, XPS characterization and optical properties of Si/SiO_2, Si/Al_2O_3 and Si/MgO co-sputtered films, Thin Sol. Films 325 (1998) 130-136.

[46] J. Tauc, R. Grigorovici, A. Vancu, Optical properties and electronic structure of amorphous germanium, Phys. Stat. Sol. 15 (1966) 627-637.

[47] M. Oliva-Ramírez, J. Gil-Rostra, F. Yubero, A.R. González-Elipe, Robust polarization active nanostructured 1D Bragg microcavities as optofluidic label-free refractive index sensor Sens. Actuat. B: Chem. 256 (2018) 590-599.

[48] R. Alvarez, C. Lopez-Santos, J. Parra-Barranco, V. Rico, A. Barranco, J. Cotrino, A.R. Gonzalez-Elipe, A. Palmero, Nanocolumnar growth of thin films deposited at oblique angles: Beyond the tangent Rule, J. Vac. Sci. Technol. B 32 (2014) 041802

[49] M. Wang, N. Pan, Predictions of effective physical properties of complex multiphase materials, Mater. Sci. Engin.: R: Reports. 63 (2008) 1-30

[50] M. Oliva-Ramírez, L. González-García, J. Parra-Barranco, F. Yubero, A. Barranco, A.R. González-Elipe, Liquid analysis with optofluidic Bragg microcavities ACS Appl. Mater. Interf. 5 (2013) 6743-6750.

[51] Z. Wu, D. Lee, M. F. Rubner, R. E. Cohen. Structural Color in Porous, Superhydrophilic, and Self- Cleaning SiO_2/TiO_2 Bragg Stacks. Small 3 (2007) 1445-1451.

[52] V. Torres-Costa, F. Agulló-Rueda, R. J. Martín-Palma, J.M. Martínez-Duart, Porous silicon optical devices for sensing applications, Opt. Mater. 27 (2005) 1084-1087.

[53] T. Jalkanen, V. Torres-Costa, J. Salonen, M. Björkqvist, E. Mäkilä, J.M. Martínez-Duart, V.P. Lehto, Optical gas sensing properties of thermally hydrocarbonized porous silicon Bragg reflectors, Opt. Express 17 (2009) 5446-5456.

[54] V. Torres-Costa, R.J. Martín-Palma, J.M. Martínez-Duart, Optical characterization of porous silicon films and multilayer filters, Appl. Phys. A 79 (2004) 1919-1923.

[55] M.F. Schubert, J. Xi, J.K. Kim, E.F. Schubert, Distributed Bragg reflector consisting of high- and low-refractive index thin film layers made of the same material, Appl. Phys. Lett. 90 (2007) 141115 1-3.

[56] W. Heiss, T. Schwarzl, J. Roither, G. Springholz, M. Aigle, H. Pascher, K. Biermann. Design and fabrication of amorphous germanium thin film-based single-material distributed Bragg reflectors operating near 2.2 μm for long wavelength applications. Prog. Quant. Electro. 25 (2001) 193-228.

[57] D. Erickson, D. Sinton, D. Psaltis, Optofluidics for Energy Applications, Nat. Photonics 5 (2011) 583-590.

[58] R.M. Parker, D.J. Wales, J.C. Gates, P.G.R. Smith, M.C. Grossel. Tracking a photo-switchable surface-localised supramolecular interaction via refractive index. J. Mater. Chem. C 6 (2016) 1178-1185.

[59] K. Mawaratari, T. Tsukahara, Y. Suqii, T. Kitamori, Extended-nano fluidic systems for analytical and chemical technologies. Nanoscale 2 (2010) 1588-1595.

[60] A. Kimberly, A. Steven, D. Jacobsen, Z. Liu, S. M. Thomas, M. Somayazulu, D. M. Jurdy, Optical reflectivity of solid and liquid methane: Application to spectroscopy of Titan's hydrocarbon lakes. Geophys. Res. Lettters 39 (2012) L04309.

[61] R.C. Luo, Y. Cao, P. Shi, C.H. Chen. Near-Infrared Light Responsive Multi-Compartmental Hydrogel Particles Synthesized Through Droplets Assembly Induced by Superhydrophobic Surface. Small 10 (2014) 4886-4894.

[62] J.G. Hu, Y.M. Zhou, X.L. Sheng. Optical diffusers with enhanced properties based on novel polysiloxane@CeO2@PMMA fillers. J. Mater. Chem. C 3 (2015) 2223-2230.

[63] V. Robbiano, G. M. Paternò, A. A. La Mattina, S. G. Motti, G. Lanzani, F. Scotognella, G. Barillaro. Room-Temperature Low-Threshold Lasing from Monolithically Integrated Nanostructured Porous Silicon Hybrid Microcavities. ACS Nano 12 (2018) 4536-4544.

[64] X.M. Kong, Y.T. Xi, P. LeDuff, E.W. Li, Y. Liu, L.J. Cheng, G.L. Rorrer, H. Tan, A.X. Wang. Optofluidic sensing from inkjet-printed droplets: the enormous enhancement by evaporation-induced spontaneous flow on photonic crystal biosilica. Nanoscale 8 (2016) 17285-17294.

[65] S.S.G. Varricchio, H. Cyrille, B. Arnaud, R. Phiulippe. Fabrication of multilayered nanofluidic membranes through silicon templates. Nanoscale 7 (2015) 20451-20459.

Graphical abstract

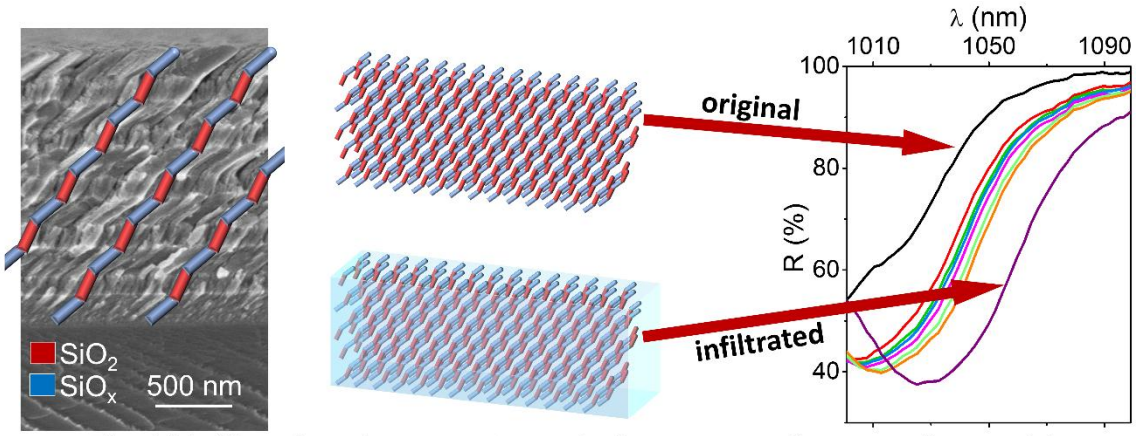

Liquid infiltration changes NIR optical response of Bragg microcavitiy

Highlights

- Reactive magnetron sputtering at oblique angle is straightforwardly used for the deposition o SiO_x thin films with controlled composition and porosity
- SiO_x thin films with x ranging from 0.4 to 1.6 have been properly characterized and their optical properties correlated with their stoichiometry and porosity
- Stacking of SiO_2 and SiO_x porous layers permits the tailored fabrication of photonic structures for the near infrared region of the spectrum
- Porous Bragg microcavities made of SiO_x and SiO_2 single layers have been used as near infrared label free optofluidic photonic sensors.